Batteries & Supercaps

Review
doi.org/10.1002/batt.202200454

Chemistry Europe
European Chemical Societies Publishing

www.batteries-supercaps.org

Research in Electrochromic Supercapacitor – A Focused Review

Tae Gwang Yun,*[a] Xi Chen,[b] and Jun Young Cheong*[c]

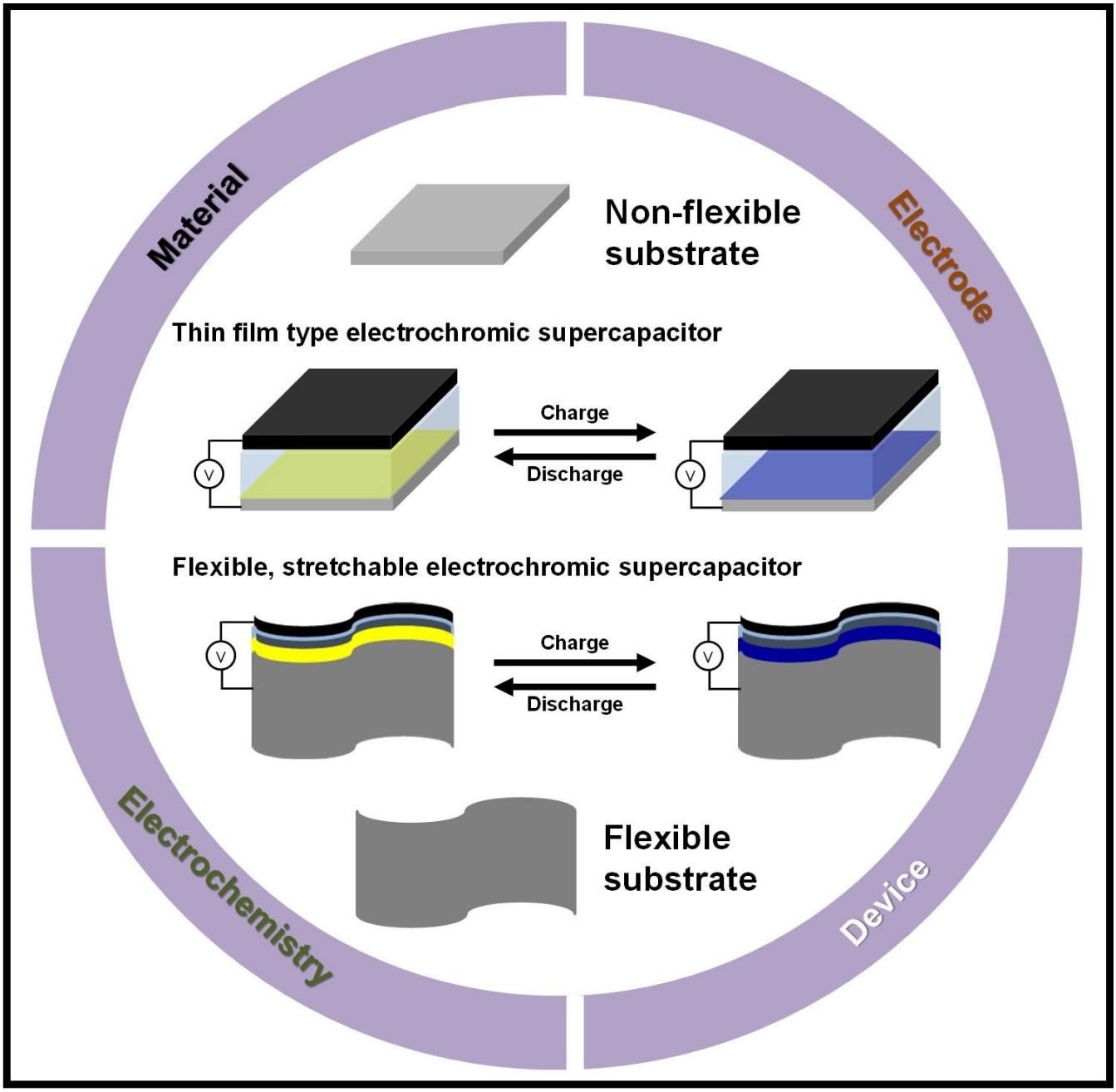

Attributed to its high safety and fast charging capabilities, supercapacitor is one of the most widely active research fields in the energy storage for last several decades. Recently, with the significant advances on the internet-of-things (IoT) technologies as well as growing market demands for wearable electronics, not only the electrochemical performance but also visual aspects of the devices become increasingly important. In this aspect, electrochromic supercapacitor has garnered significant attention in the last decade, which exhibits both color transition and reversible charge/discharge. So far, although some works have been devoted to investigating on the materials and/or components of electrochromic supercapacitor, none of the works have carefully investigated and analyzed the history, research progress, and future directions for electrochromic supercapacitor. In this review, the research progress and advances in the electrochromic supercapacitor are summarized, as well as suggestion for future directions for the electrochromic supercapacitor, which makes an early projection for future research on electrochromic supercapacitor.

1. Introduction

Renewable energy continuously produces electricity through converting the flow of nature resources that occurs infinitely in nature into electrical energy. Therefore, it is attracting attention as a next-generation eco-friendly energy generation system that can replaces fossil fuels causing environmental pollution. Renewable energy has developed as (1) eco-friendly large-scale energy converting system,[1–3] and (2) small power generating system for IoT and wearable electronic devices.[4,5] In particular, the demand for small power generating system is rapidly increased by applied as power supply for wearable electronic device, which are utilized in integration with healthcare technology.[6–9]

Alongside the sustainable energy conversion, sustainable energy storage system has garnered much attention, and aqueous energy storage system has attracted a considerable attention due to its safety merits.[10–13] Based on the recent evaluation,[14] aqueous energy storage system has been rarely researched before 1995; its research gradually increased until 2010s; and it was actively researched after 2010s. Amongst various aqueous energy storage system, supercapacitor has been researched in various academia and laboratories,[15–19] because it can allow considerable safety as well as superfast charging of electrode, resulting in superior rate capabilities. Different types of supercapacitors, ranging from micro-supercapacitors[20–22] to flexible supercapacitors,[23–25] have been researched, with many citations across the energy fields. The use of supercapacitor has recently also been extended to wearable electronics,[26,27] where simultaneous consideration on not only the electrochemical performance but also the visual aspect is now indispensable.

Electrochromic supercapacitor is one of the most interesting forms of supercapacitor, as it allows the energy storage and color transition simultaneously.[28] It has recently garnered much attention, and many follow-up works have already been published. In line with the aqueous energy storage system, significant research works and advances took place after 2010, and various research works ranging from the material synthesis to demonstration took place. Nevertheless, no focused review on the research trend of electrochromic supercapacitor and suggestion for the future direction for electrochromic supercapacitor are yet suggested, which are important aspects to be considered. In this review, we thoroughly summarize and analyze some of the research trends related to the electrochromic supercapacitor, current state-of-the-art, and the future research perspectives for electrochromic supercapacitor. It is expected that this review will establish a milestone for future research related to electrochromic supercapacitor, which has a broad readership.

2. Materials/Electrochromism, Setup, and Electrochemical Analysis of Electrochromic Supercapacitor

2.1. Types of materials and progress in materials

Electrode materials for electrochromic supercapacitor can be generally classified into the types of materials, such as polymers,[29] oxides,[30] hydroxides,[31,32] and combination of them. Depending on the type of electrode materials, each of them exhibits unique electrochemical properties, so careful investigation is necessary. In general, electrochromism occurs during the insertion/extraction process of electrons and ions (H^+, Li^+) in a material. Electrochromic materials are largely transition metal oxides such as tungsten, nickel, and vanadium, metal complexes such as Prussian blue, metal hydroxides such as $Co(OH)_2$ and $Ni(OH)_2$, and polymers such as viologen/polypyrrole/polyaniline. Transition metal oxides and metal hydroxides are clearly divided into cathodic coloration materi-

[a] Prof. T. G. Yun
Department of Materials Science and Engineering
Myongji University
Yongin, Gyeonggi 17058 (Republic of Korea)
E-mail: ytk0402@mju.ac.kr
[b] Prof. X. Chen
Department of Earth and Environmental Engineering
Columbia University
New York City, NY 10027 (USA)
[c] Dr. J. Y. Cheong
Bavarian Center for Battery Technology (BayBatt) and Department of Chemistry
University of Bayreuth
Universitätsstraße 30, 95447 Bayreuth (Germany)
E-mail: Jun.Cheong@uni-bayreuth.de

als colored by ion intercalation and anodic coloration materials colored by ion extraction. Reductive coloring materials include TiO_2, MoO_3, WO_3 (blue, wavelength 450–495 nm), Nb_2O_5 (yellow, 500–530 nm), and oxidation coloring materials include Cr_2O_5, MnO_2, FeO_2, (yellow, 500–530 nm). nm), CoO_2, NiO_2 (brown, 590–620 nm). Transition metal oxides have excellent durability and can be used for a long time. However, it is difficult to implement various colors, and the discoloration rate and discoloration efficiency are low due to low electrical conductivity. In contrast, metal complexes and conductive polymers are not clearly divided into reduction-colored and oxidized-colored materials. Therefore, various colors can be implemented, and the discoloration rate and discoloration efficiency are excellent due to high electrical conductivity, but it is weak against heat and has low efficiency in large-area processes.

The electrochemical energy storage mechanism of electrochromic materials varies depending on the type of material. First, transition metal oxides store charge based on intercalation pseudocapacitance reactions. Typically, WO_3-based electrochromic materials store charge by intercalating cations in a monoclinic or hexagonal crystal structure (Figure 1a).[33] Through CV profiles, the porous structure (mesoporous WO_3, m-WO_3) significantly increases the specific and volumetric capacitance (109 F g^{-1}). In particular, since WO_3 has a structure that efficiently absorbs hydrogen ions, energy storage efficiency is maximized in acidic electrolytes. Therefore, by using the porous transition metal oxide nanostructure, it is possible to maximize electrochromic and electrochemical energy storage efficiency. Metal complexes also store charge by the same intercalated pseudocapacitance mechanism as transition metal oxides. Typically, when ions are inserted/extracted from Prussian blue (PBAs, $NaM[Fe(CN)_6]_y$), the redox reaction of transition metal M and the redox reaction of Fe^{2+}/Fe^{3+} occur in pairs (Figure 1b).[34] However, it has very low theoretical capacity (170 mAh g^{-1}) and reversible capacity (70–100 mAh g^{-1}), so it is not suitable for electrochromic supercapacitors. Metal hydroxides store charges based on a redox pseudocapacitance reaction in which faradaic charge transfer occurs when ions in the electrolyte are electrochemically adsorbed on or close to the surface of an electrode. The oxidation/reduction reaction of Ni^{2+}/Ni^{3+} is formed in pairs. Metal hydroxides exhibit battery-type CV profiles (Figure 1c),[35] with very high theoretical and reversible capacities (2000–3000 F g^{-1}). Co^{2+}/Co^{3+} states were clearly shown in the CV profiles of $Co(OH)_2$, and the maximum capacity was 2646 F g^{-1}. Therefore, electrochromic supercapacitors based on metal hydroxides can maximize electrochemical performances. Conductive polymers improve charge transfer kinetics by supplementing the low electrical conductivity of existing electrochromic materials. Improved charge transfer kinetics significantly increase coloration response and efficiency. Con-

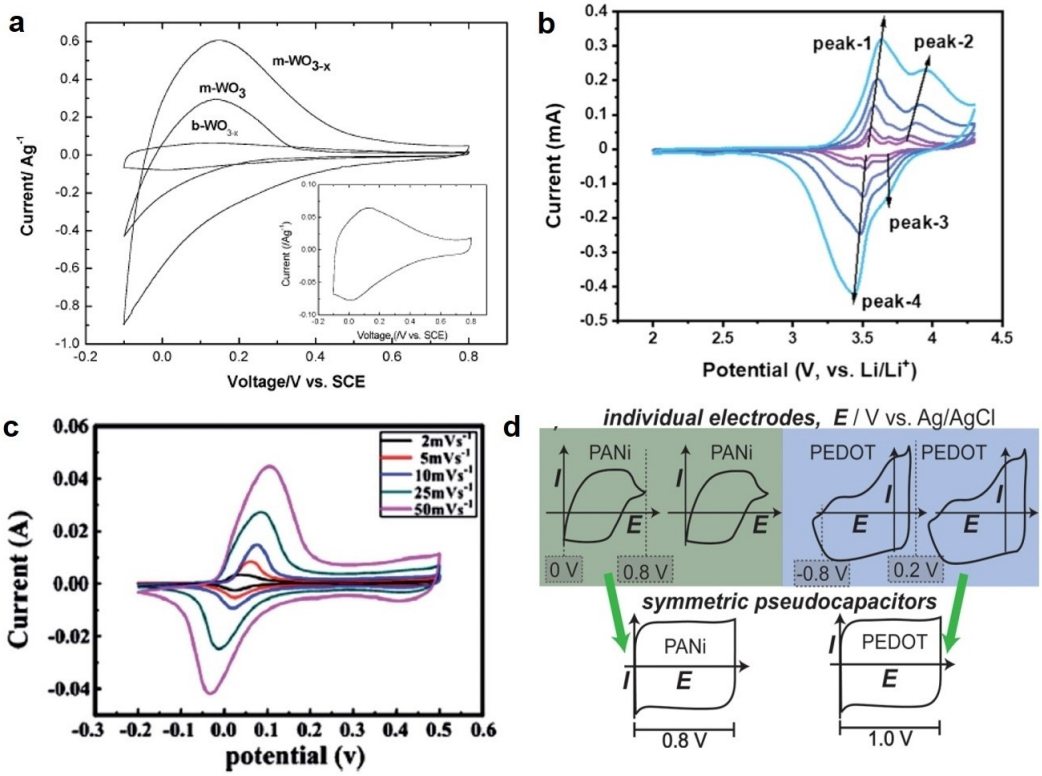

Figure 1. a) CV curves of different kinds of WO_3-based materials. Reproduced with permission from Ref. [33]. Copyright (2011) Royal Society of Chemistry. b) CV curves of Prussian blue at different scan rates, characterized by four different peaks. Reproduced with permission from Ref. [34]. Copyright (2021) The Authors. Advanced Energy and Sustainability Research published by Wiley-VCH. c) CV curves of electrodeposited $Co(OH)_2$ on graphene at various sweep rates. Reproduced with permission from Ref. [35]. Copyright (2014) Royal Society of Chemistry. d) CV curves of PANi and PEDOT polymers and overall CV curves with different voltage range. Reproduced with permission from Ref. [36]. Copyright (2016) American Chemical Society.

ductive polymers store charge based on the same redox pseudocapacitance mechanism as metal hydroxides. The CV profiles of representative conductive polymers, polyaniline (PANi) and PEDOT:PSS, are shown in Figure 1(d).[36] Generally, PANi, which is positively polarized, has a charge-discharge reaction within a voltage range of 0–0.8 V based on the Ag/AgCl reference electrode in a neutral aqueous electrolyte. On the other hand, PEDOT:PSS, which is negatively polarized, has a charge-discharge reaction within a voltage range of −0.8–0.2 V in a neutral aqueous electrolyte. The maximum capacities of both PANi and PEDOT:PSS appear in the range of 300–400 $F g^{-1}$. Therefore, conductive polymers are suitable for various discoloration reactions and high-capacity electrochromic supercapacitors.

Up to the present, significant research progress has been present for material development for electrochromic supercapacitor. More significant advances were made on the composition and properties of material, while synthetic method had minor changes in the kinds of chemical precursors used. For example, Song et al. reported on the use of chalcogenoviologen-based ionic liquid ($[C_6EVC_6][TFSI]_2$, E=S, Se, Te) and ferrocene-based ionic liquid ($[FcC_{11}ImC_1][TFSI]$),[37] synthesized by multi-step chemical reactions. Yue et al. employed novel conjugate polymer based on thienoisoindigo,[38] by utilizing tris(thienothiophene) and thieno [3,2-b]- thiophene. Through Stille reaction, purple colored polymer was obtained and used as purple-to-transparent electrochromic materials. Along with advances in chemical compositions of materials, morphology tuning of materials was also investigated in detail. Ma et al. discovered that morphology tuning can significantly affect the electrochromic performance, where WO_3 nanorod array films exhibited the larger transmittance modulation than WO_3 nano brick film.[39] This is because larger tunnels and higher active surface area were available for WO_3 nanorod array films, where clear correlation between morphology and performance was obvious. Choi et al. investigated microstructure control of NiO for electrochromic performance,[40] which drew similar conclusions that rationally designed structure/morphology can greatly influence the electrochromic performance. Nano-sized, submicron-sized, and micron-sized NiO powders were compared for electrochromic performance and micron-sized NiO powders showed the optimal performance because it showed the smallest crystallite size. Synthesis of novel material based on new chemical precursor or modified synthetic method and careful optimization on its morphology can greatly improve and advance the electrochromic properties and performances.

2.2. Electrode preparation

The criteria for evaluating the electrochromic performance of electrochromic devices include coloration efficiency, coloration contrast (optical density), and response time. Specifically, coloration contrast (optical density, OD) is a physical quantity expressed as log of transmittance change in bleached (T_b) and colored state (T_c). Coloration efficiency (η) is a physical quantity that expresses the coloration contrast that changes with the applied unit charge density (Q). The higher the coloration efficiency, the higher the change in transmittance per unit current. Response time means the speed at which the coloration reaction occurs, and is closely related to the electrical conductivity of the electrode.

$$\Delta(\mathrm{OD}) = \log((T_b)(T_c)^{-1}) \quad (1)$$

$$\eta = \Delta(\mathrm{OD})(Q)^{-1} \quad (2)$$

Electrochromic devices need to maximize coloration contrast and coloration efficiency, so it is necessary to develop active materials with low density based electrode with maximized transmittance, a transparent current collector with high electrical conductivity and a transparent electrolyte. For the current collector, glass-based transparent electrodes with a transmittance of over 90% are applied. Representatively, fluorine doped tin oxide (FTO), indium doped tin oxide (ITO), and metal nanowires electrodes are used as current collectors. However, glass-based electrochromic devices are fragile and do not have flexible-stretch characteristics, so the application range is limited. So, recently, current collectors using transparent flexible-extension substrates such as transparent polymer, metal mesh and cellulose fiber have been developed.

2.3. Types of supercapacitor and electrochemical analysis

Supercapacitor is a non-faradic reaction-based electrical double layer capacitor (EDLC) that stores charge by forming a double layer on the surface of the electrode and stores charges based on oxidation/reduction reactions caused by the Faradic reaction occurring on the surface of the electrode. It is classified as a pseudocapacitor that in general, it is classified as capacitive behavior if EDLC reaction is dominant, pseudocapacitive behavior if faradaic and EDLC reaction are mixed, and battery behavior if faradaic reaction is dominant, pseudocapacitive behavior if the pseudocapacitor and EDLC reaction are mixed, and battery-type (Faradic behavior) if the pseudocapacitor reaction is dominant (Figure 2).[41] In order to develop supercapacitors with electrochromic reactions, pseudocapacitive or battery-type active materials are absolutely necessary.

3. Conventional Film-based Electrochromic Supercapacitor

3.1. Single component active materials

To start with, the electrochromic supercapacitor was firstly reported by Wei et al,[42] which is composed of V_2O_5. Figure 3(a) shows the scanning electron microscopy (SEM) images of mesoporous V_2O_5 grown on fluorine tin oxide (FTO) substrate. The V_2O_5 was fabricated by electrodeposition process, allowing the free-standing structure. The mesoporous V_2O_5 was readily transformed into double-gyroid morphology by self-assembly.

Review
doi.org/10.1002/batt.202200454
Chemistry Europe
European Chemical Societies Publishing

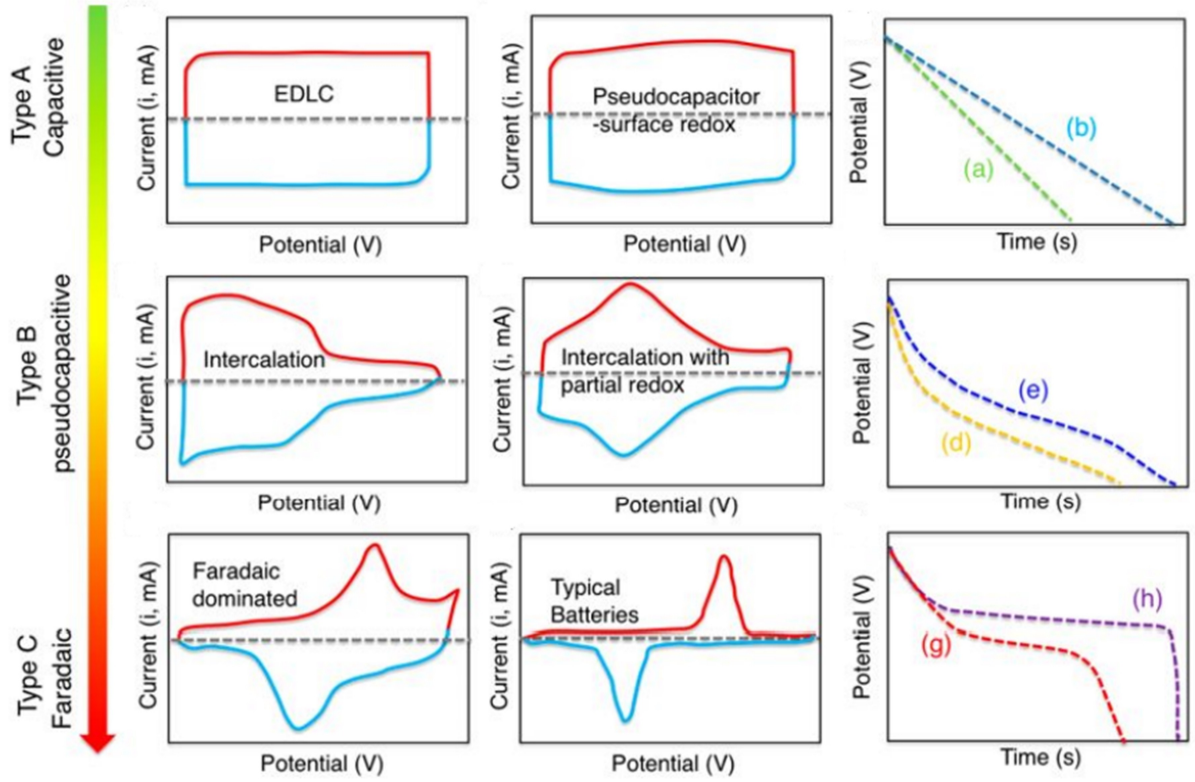

Figure 2. Transition from capacitive reaction (Type A) to faradaic reaction (Type C), with varied CV curves and corresponding galvanostatic profiles. Reproduced with permission from Ref. [41]. Copyright (2020) American Chemical Society.

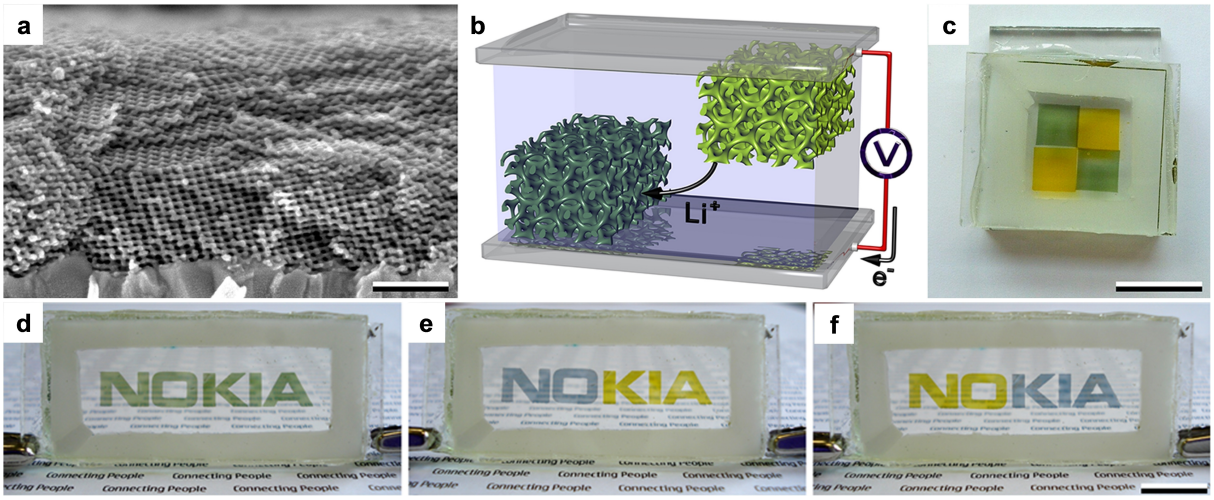

Figure 3. a) Cross-section SEM images of mesoporous V_2O_5 film grown on FTO substrate. b) Schematic illustration of the electrochromic supercapacitor design. c) Photograph of a fully transparent electrochromic supercapacitor. Photograph of a supercapacitor at d) discharged state (0 V) and e,f) charged state (3.5 V) with reverse polarity. Reproduced with permission from Ref. [42]. Copyright (2012) American Chemical Society.

Figure 3(b) depicts the schematic illustration of the supercapacitor consisting of two laterally offset double-gyroid structured electrodes. The actual photograph (Figure 3c) of such supercapacitor, where an oxidized yellow top electrode is laterally offset from the reduced green bottom electrode, with a thermoplastic gasket spacer. The double-gyroid structure is highly ordered, with 11.0 nm wide struts and high specific surface-to-volume ratio. As a result, the supercapacitor shows a high specific capacitance of 155 $F g^{-1}$ and a consistent color change from green/gray to yellow. Such visual demonstration is presented in Figure 3(d–f), where the supercapacitor was discharged at 0 V and again charged at 3.5 V with reverse polarity. This work was an early report on adopting film-based electrodes for electrochromic supercapacitor, which opened up the possibility to utilize color transition to identify the state of charged/discharged state. In addition to V_2O_5, other metal

oxides such as NiO[43,44] and WO_3[45] were also investigated in detail. Followed by the initial publication in 2012, Steiner group further employed a unique 3D nanotubular gyroid network composed of NiO, which was utilized for electrochromic supercapacitor.[43] Thermal oxidation turns Ni into NiO, which then can be employed as an active material for electrochromic supercapacitor. In another study, Cai et al. reported on the growth of uniform NiO nanoparticles on substrates with a low cost solvothermal method.[44] It exhibits excellent capacitance (1386 $F g^{-1}$) at 1.0 $A g^{-1}$ as well as superior rate capabilities, while also demonstrating large optical modulation (63.6% at 550 nm) and high coloration efficiency (42.8 cm^2 C^{-1} at 550 nm). Yun et al. combined WO_3 and Li-doped ionic gels for dual-functional supercapacitor,[45] where simultaneous color transition and charging/discharging took place at the voltage range of 0 and −1.5 V.

3.2. Composite active materials

Composites of multiple active materials were also heavily researched to incur synergistic effects between various active materials present for supercapacitor and electrochromic properties. Other conventional transition metal oxides including the ones mentioned above[46–50] were also researched (either for electrochromic, supercapacitor, or both of them), where materials having the characteristics of electrochromic transition and supercapacitor performance have been used widely. Since its initial report on utilizing metal oxide for electrochromic supercapacitor, other kinds of materials have been delved into for an electrochromic supercapacitor. Li et al. fabricated micro-supercapacitor composed of MXene and conducting polymer,[51] which yielded extremely 5-fold areal capacitance and high rate capabilities (2.4 mF cm^2 at 10 mV s^{-1}). Such enhancement is attributed to the high electric conductivity of conducting polymer in comparison with metal oxides and uniform distribution of MXene in the bottom layer. Charging and discharge characteristics of such energy-storing functional photovoltaic devices are illustrated in Figure 4(a),[52] where charging time for this energy-storing functional photovoltaic devices is approximately 91 s. Depending on the areal current densities (0.04, 0.08, 0.12, 0.16, and 0.20 mA cm^{-2}), there is a varied discharge time, where it decreases with respect to increased areal current densities. The relationship between the areal capacitance and the current density is also presented in Figure 4(b), where it is inversely proportional to the increased current density. Color transition during charging and discharging process (Figure 4c and d) shows that at different voltages, different color exists and it can undergo color transitions in a reversible manner. For a realistic application, electrical circuits related to the photovoltaics and energy storage system are schematically illustrated in Figure 4(e), with digital camera images of where each of the component lies in. This work provided an innovative design that combined electrochromic supercapacitor together with photovoltaics, which established an important milestone in how the idea can be realized in a real product scale. Combination of various active materials were also implemented in tried in recent literatures. Ezhilmaran et al. developed an aluminum electrochromic supercapacitor composed of TiO_2/MoO_3, which exhibited good coloration efficiency (128 $cm^2 C^{-1}$) and transmittance change (54%).[53] Layered double hydroxides were also combined with metal oxides for electrochromic supercapacitor. Liu et al. reported Ni/Co layered double hydroxide together with ZnO for electrochromic supercapacitor device,[54] which exhibits high energy and power density (7.7 μWh cm^{-2} and 375.0 μW cm^{-2}) and good optical properties (such as large transmittance modulation of 63% at 660 nm). Mohanadas et al. combined reduced graphene oxide (rGO) together with NiO, V_2O_5, which resulted in the bifunctional asymmetric electrochromic supercapacitor with unique performances and properties.[55] It exhibits an excellent cycling stability (92.2% over 4000 cycles) as well as maximum

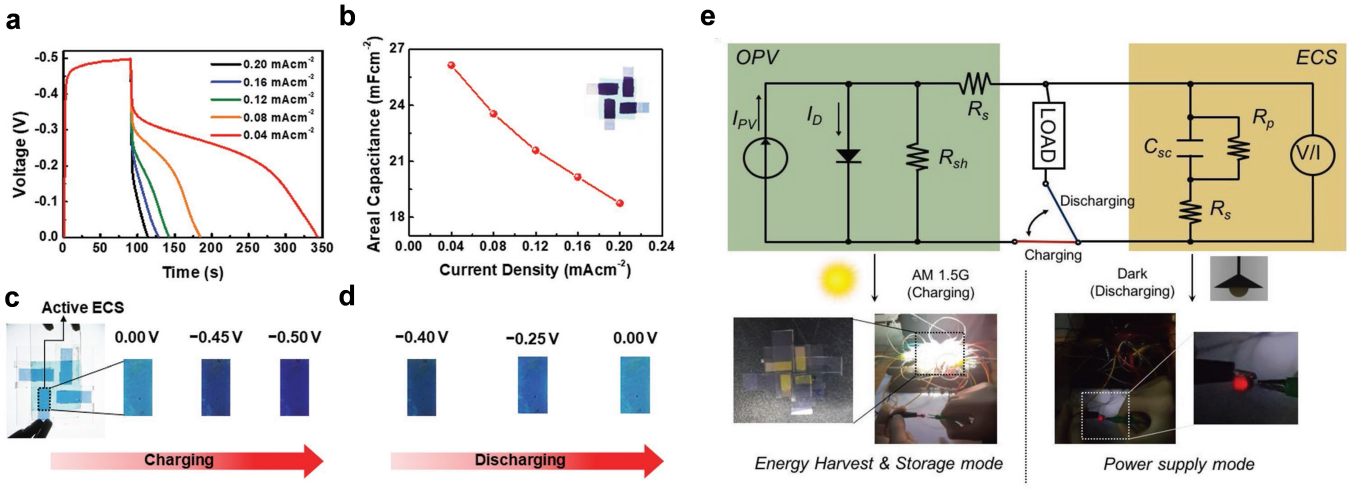

Figure 4. a) Galvanostatic charge and discharge profiles and b) corresponding areal capacitance for photovoltaic-electrochromic supercapacitor. Changes in colors during c) charging and d) discharging process. e) Electrical circuits corresponding to the photovoltaic-electrochromic supercapacitor and energy harvesting/storage mode (charging) and power supply mode (discharging). Reproduced with permission from Ref. [52]. Copyright (2020) Wiley-VCH.

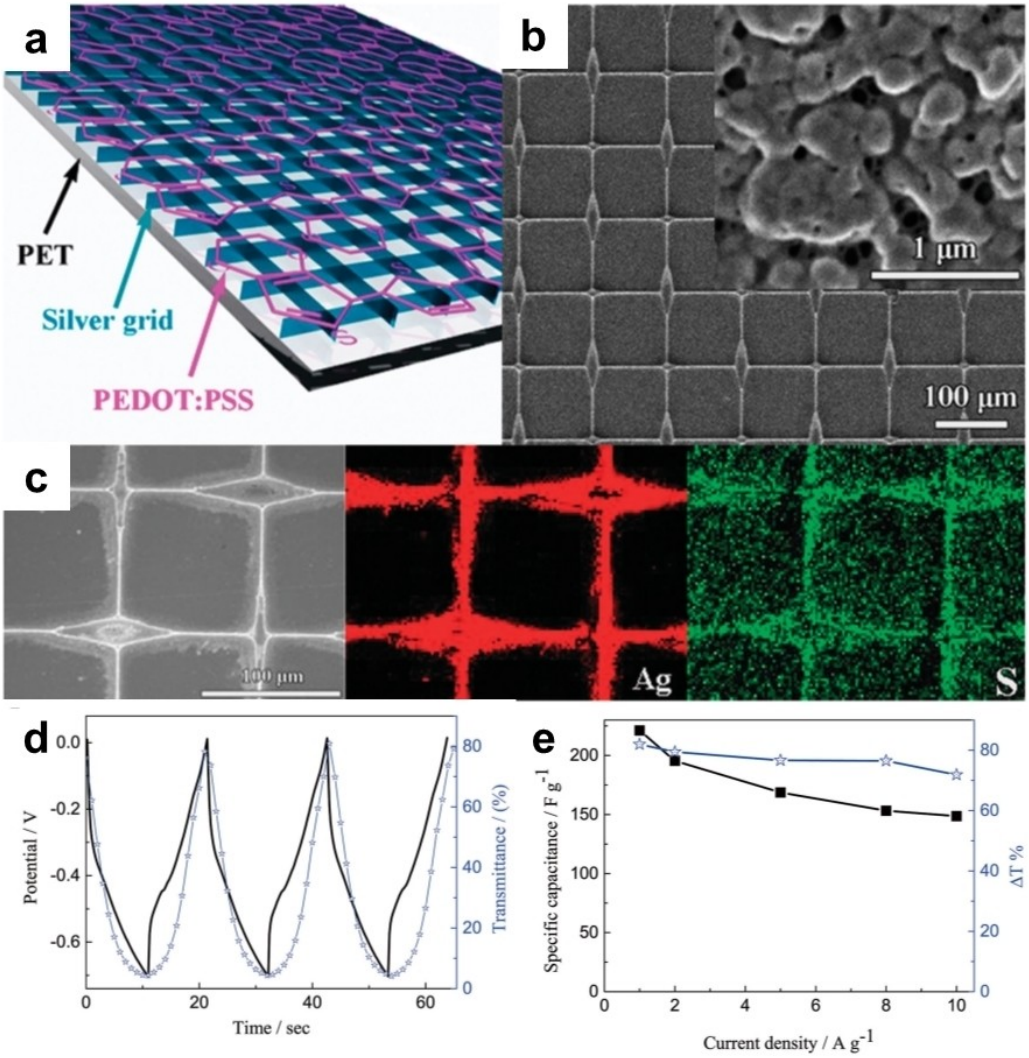

Figure 5. a) Schematic illustration on the silver/PEDOT:PSS hybrid film and the location of each component. b) SEM images in low and high magnification of the silver/PEDOT:PSS hybrid film. c) EDS mapping of Ag and S for silver/PEDOT:PSS hybrid film, demonstrating the uniformity of elements across the hybrid film. d) Galvanostatic charge and discharge profile at the voltage window of 0 to −0.7 V and transmittance trend. e) Specific capacitance and transmittance changes of the WO_3 on the silver/PEDOT:PSS hybrid film. Reproduced with permission from Ref. [69]. Copyright (2016) Wiley-VCH.

specific energy of 41.4 Wh kg^{-1}, which is unprecedented for electrochromic supercapacitor having one component of these composites. As such, synergistic effects were profoundly found in combining two or more components, and therefore, a number of hybrid materials were applied for electrochromic and/or supercapacitor applications, some of which include $W_{18}O_{49}$/rGO composite films,[56] Mo-doped crystalline/amorphous WO_3,[57] NiCo-mixed hydroxide nanosheets,[58] poly(1H-benzo[g]indole)/TiO_2 nanocomposite,[59] $NiMoO_4$@$NiMnCo_2O_4$ heterostructure,[60] rGO/NiO heterostructure,[61] poly(indole-6-carboxylicacid)/WO_3 nanocomposites,[62] oligoaniline-functionalized polysiloxane/Prussian blue composite,[63] and poly(indole-6-carboxylicacid)/TiO_2.[64] Amongst them, some of metal oxide-conductive polymer composites need to be discussed more in detail.[59,62,64] Wang et al. synthesized poly(1H-benzo[g]indole)/TiO_2 nanocomposite via hydrothermal synthesis and electrochemical polymerization,[59] where synergistic effects of conductive polymer and TiO_2 were expected based on the matched energy level. With the addition of TiO_2, capacitance significantly increased, which highlights the advantage of combining conductive polymer with metal oxide. Similarly, Li et al. combined poly(indole-6-carboxylicacid) with WO_3 to render synergistic effects between conductive polymer and metal oxide.[62] As both of these components have effective energy level matching. Especially, unique core-shell nanorod structure of poly(indole-6-carboxylicacid)/WO_3 exhibits a large optical modulation of 62% and specific capacitance of 13.69 mF cm^{-2}, which are outstanding electrochromic performance. Poly(indole-6-carboxylicacid) was also combined with TiO_2,[64] which also exhibited outstanding electrochromic/electrochemical performance. Due to synergistic effect between poly(indole-6-carboxylicacid) and TiO_2, high specific capacitance of 23.34 mF cm^{-2} and coloration efficiency of 124 cm^2 C^{-1} were achieved. The overall electrochemical as well as electrochromic performance of active materials were compared and summarized in Table 1, which shows varied physicochemical

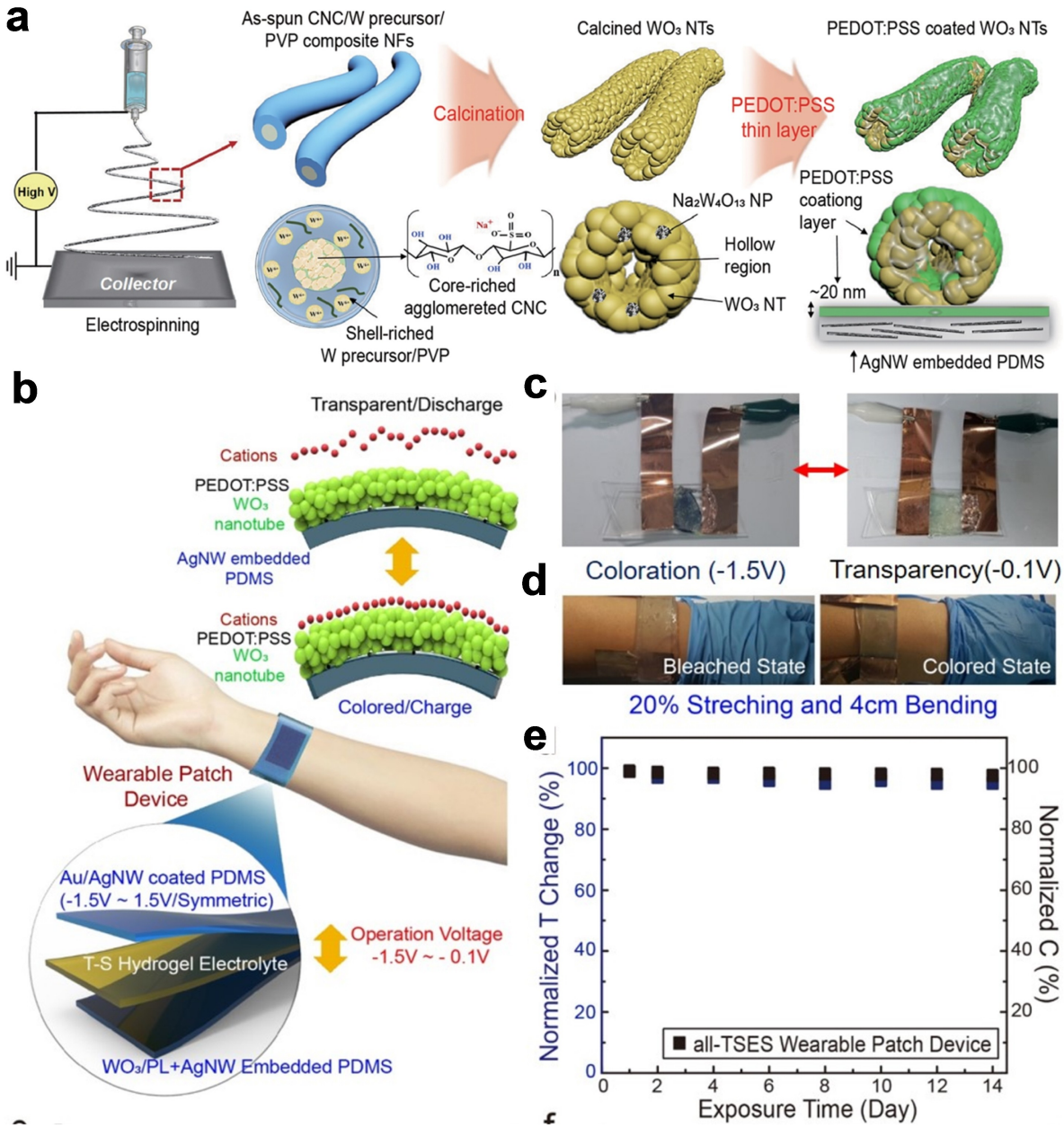

Figure 6. a) Schematic illustration on the fabrication process of WO_3 nanotubes and PEDOT:PSS layer. b) Schematic illustration of wearable patch device containing WO_3 nanotubes and PEDOT:PSS layer. c) Real image of bleached and colored state of a wearable patch device. d) Demonstration of wearable patch device. e) Normalized coloration contrast change and capacitance retention of a wearable patch device after exposure in ambient conditions for 14 days. Reproduced with permission from Ref. [78]. Copyright (2019) American Chemical Society.

properties depending on the current density (or scan rate), type of electrolyte used, concentration of salt, and active materials used.

3.3. Combination with other devices

Furthermore, more research works delved into the efficacy of employing electrochromic supercapacitor coupled with other energy storage/conversion devices. Xie et al. combined dye sensitized solar cells with WO_3 based electrochromic devices, which yielded high areal capacitance and reversible color changes.[65] Within a small current density of 0.106 mA cm^{-2}, it can achieve high areal capacitance of 0.022 F cm^{-2}, which is considerably high. It can be demonstrated that dye sensitized solar cell could be employed as a power supply to operate electrochromic supercapacitor. In another study,[66] Wang et al. integrated energy storage and electrochromic function in one single device, which showed high stability in electrochromic function and electrochemical performance. Some research progress in the measurement methods was also present, where Zhu et al. reported on employing optical spectra, which resulted in precisely controlled electrical energy storage.[67]

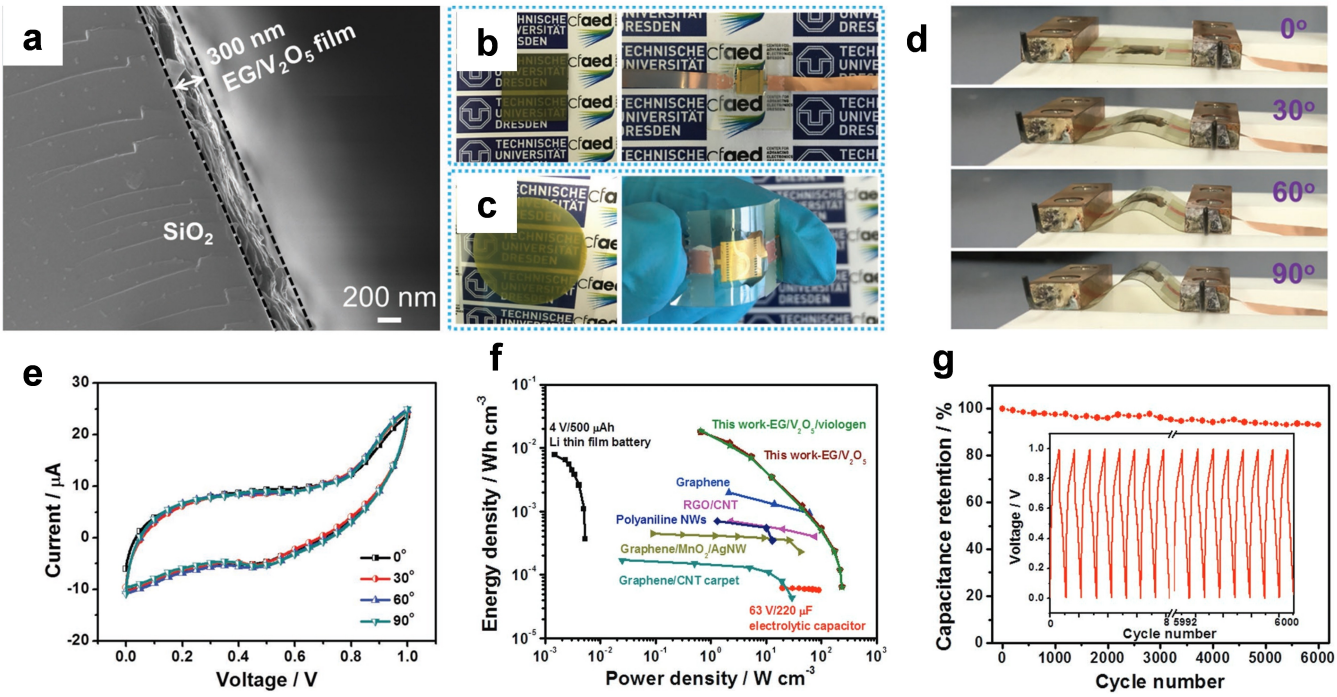

Figure 7. a) SEM image of glass-supported EG/V_2O_5. Digital photos of EG/V_2O_5 MSC devices (size: 1.5 cm × 1 cm) on b) glass and c) PET substrates. d) Optical photos of the EG/V_2O_5-fMSC with bending angles. e) Similarity in CV curves of the EG/V_2O_5-fMSC under different bending angles. f) Ragone plots of this work with previously reported literatures. g) Cycling stability over 6000 cycles. Reproduced with permission from Ref. [81]. Copyright (2017) Wiley-VCH.

Table 1. Summary of electrochemical performance on various types of thin film electrochromic supercapacitor.

Active materials	Electrolyte	Capacitance	Coloration contrast	Cycling stability	Ref.
NiO	1 M KOH in H_2O	1386 F g^{-1} at 1.0 A g^{-1}	63.6% at 550 nm	78.5% after 5000 cycles	[44]
NiO	1 M KOH in H_2O	2.08 F cm^{-2} at 1 mA cm^{-2}	41.08% at 650 nm	86.7% after 15000 cycles	[48]
WO_3—V_2O_5	1 M $LiClO_4$ in polypyrrole carbonate	38.75 mF cm^{-2} at 0.5 mA cm^{-2}	60% at 700 nm	78.5% after 5000 cycles	[49]
Ni_xV_y oxide	2 M KOH in H_2O	139 F g^{-1} at 1.0 A g^{-1}	68% at 630 nm	91.95% after 2000 cycles	[50]
MXene-PEDOT	1 M PVA/H_2SO_4 in H_2O	2.4 mF cm^{-2} at 10 mV s^{-1}	54% at 550 nm	90% after 10000 cycles	[51]
TiO_2/α-MoO_3	0.1 M $AlCl_3$ in H_2O	218.8 mF cm^{-2} at 0.1 mV cm^{-2}	54%	91.6% after 2000 cycles	[53]
ZnO@Ni/Co layered double hydroxide	1 M KOH/PVA in H_2O	24.6 mF cm^{-2} at 0.5 mA cm^{-2}	56% at 550 nm	93.5% after 1500 cycles	[54]
NiO/V_2O_5/rGO	1 M KCl	1265.5 F g^{-1} at 5 mV s^{-1}	71.4%	92.2% after 4000 cycles	[55]
Mo-doped WO_3	$LiClO_4$/PC	39.2 mF cm^{-2} at 0.1 mA cm^{-2}	67.8% at 633 nm	72.8% after 1500 cycles	[57]
Poly(1H-benzo[g]indole)/TiO_2	$LiClO_4$ in acetonitrile	13.2 mF cm^{-2} at 0.1 mA cm^{-2}	35.3% at 625 nm	86% after 3000 cycles	[59]
$NiMoO_4$@$NiMnCo_2O_4$	6 M KOH in H_2O	2706 F g^{-1} at 1.0 A g^{-1}	41.5% at 535 nm	97.8% after 50000 cycles	[60]
rGO/NiO	1 M KOH in H_2O	269 mF cm^{-2} at 0.5 mA cm^{-2}	53% at 630 nm	Almost 100% after 1000 cycles	[61]
Poly(indole-6-carboxylicacid)/WO_3	H_2SO_4—PVA	13.69 mF cm^{-2} at 0.05 mA cm^{-2}	62% at 625 nm	86% after 3000 cycles	[62]
Poly(indole-6-carboxylicacid)/TiO_2	$LiClO_4 \cdot 3H_2O$, PMMA, CH_3CN, and PC	23.34 mF cm^{-2} at 0.25 mA cm^{-2}	36% at 720 nm	91% after 5000 cycles	[64]

4. Flexible Electrochromic Supercapacitor

4.1. Flexible electrochromic supercapacitor

In addition to simply introducing various active materials that can undergo color transition and supercapacitor performance, more advances in the structure of electrochromic supercapacitor were present, namely making it flexible or stretchable. Various kinds of flexible-stretchable electrochromic supercapacitor were devised and further tested for electrochemical performance, even for some of the electrode materials mentioned above.[56] Chen et al. introduced the concept of "fiber-shaped" electrochromic supercapacitors, capable of bending and weaving.[68] Electrodeposition of polyacrylonitrile

(PANI) onto the sheets of aligned carbon nanotubes (CNTs) was carried out, and the fiber-shaped electrochromic supercapacitor has a color transition from light green (at 0 V) to blue-ish green (at 1 V), while showing the maintenance of capacitance even after 100 stretching cycles. Interesting transparent electrochromic supercapacitor composed of conductive silver grid and poly(3,4-ethylenedioxythiophene) polystyrene sulfonate (PEDOT:PSS) was devised and introduced by Cai et al.,[69] which exhibited high coloration efficiency (124.5 $cm^2 C^{-1}$). Schematic illustration of silver/PEDOT:PSS hybrid film is presented in Figure 5(a), where silver grid was placed on top of PET substrate and PEDOT:PSS is deposited onto the silver grid. SEM images in low and high magnification (Figure 5b) clearly show the uniformity of both silver grid and PEDOT:PSS, and silver particles are coated by the PEDOT:PSS. Uniformity of coating can further be verified by Figure 5(c), where it has uniform distribution of both Ag and S, representing the silver grid and PEDOT:PSS. Galvanostatic charge and discharge profile and transmittance change were examined in Figure 5(d), where reversible reaction was clear. The dependence upon the capacitance and the current density was further examined in Figure 5(e), where silver/PEDOT:PSS hybrid film maintains good capacitance even at high current density (10 $A g^{-1}$). In addition to the flexibility, the bendable characteristics of electrochromic supercapacitor was investigated, together with the electrochromic properties. Yun et al. reported on the electrochromic supercapacitor based on the photo-responsive smart coloration,[70] which also showed outstanding bending characteristics. Additionally, ultra-flexible bifunctional electrochromic supercapacitor was devised and fabricated by Ginting et al.[71] which combined Ag nanowire together with PEDOT:PSS, similar to the work previously mentioned.[69] In terms of the synthetic methods, a simple method such as spray coating was employed to deposit electrochromic donor-acceptor polymer (poly[4,7-bis(3,6-dihexyloxy-thieno[3,2-b]thiophen-2-yl)]-benzo[c][1,2,5]thiadiazole) onto the flexible ITO/PET substrate, which was newly synthesized and yielded considerable capacitance as well as color transitions.[72] Similar with above-mentioned system but with different compositions, Shen et al. combined Ag nanowire together with WO_3 films, which also showed unique electrochromic properties and considerable capacitance.[73] It exhibited an areal and gravimetric capacitance of 13.6 $mF cm^{-2}$ and 138.2 $F g^{-1}$, with a coloration efficiency of 80.2 $cm^2 C^{-1}$. Another material engineering that was employed was also the stacking. Grote et al. reported on the cobalt-nickel hydroxide-coated reduced graphene oxide nanosheets, which were stacked with each other.[74] Such stacked composites exhibited pseudocapacitive charge storage behavior as well as high rate capabilities, desirable for electrochromic supercapacitor. In addition to the ones described above, other flexible electrochromic supercapacitor such as carbon nanotubes/Au/polypyrrole/PET,[75] polyaniline films,[76] and ladder-like donor-acceptor polymers.[77]

4.2. Stretchability of flexible electrochromic supercapacitor

In addition to the flexibility of the electrochromic supercapacitor, the stretchability of electrochromic supercapacitor has also been investigated widely. Yun et al. devised and fabricated a unique all-transparent stretchable electrochromic supercapacitor, which can also be employed for the wearable patch device.[78] Schematic illustration on the electrospinning setup, calcination to fabricate WO_3, and PEDOT:PSS thin layer coating is presented in Figure 6(a), where PEDOT:PSS thin layer is expected to cover the surface of WO_3 nanotubes. Schematic illustration on the demonstration of how this electrochromic supercapacitor can be used as a wearable patch is presented in Figure 6(b). Upon discharge process, the color becomes transparent; upon charge process, the color becomes dark blue. With the operation voltage of −1.5 V to −0.1 V, it can reversibly operate and undergo reversible color transition, where the users will know the state of the device (whether it is charge and/or discharged). Such visualization is clearly seen in Figure 6(c) and reversible electrochromic and electrochemical properties are demonstrated even under 20% stretching and 4 cm bending (Figure 6d). Even after the exposure to air for 14 days, overall coloration contrast and capacitance change retain in a substantial manner (Figure 6e). Adding the stretchable and flexible functionalities together can result in an outstanding electrochromic supercapacitor, some of which include vertical gold nanowires and polyaniline[79] and WO_3 nanoparticles on the elastomer.[80]

Some novel forms of flexible electrochromic supercapacitor were also devised and fabricated. Zhang et al. combined one-dimensional V_2O_5 and two-dimensional V_2O_5 and two-dimensional exfoliated graphene for stimuli-responsive micro-supercapacitors,[81] which also exhibit flexible characteristics. SEM image of V_2O_5/exfoliated graphene composite is presented in Figure 7(a), where it has a 300 nm thick V_2O_5/exfoliated graphene coated onto the SiO_2 substrate. Visual images of V_2O_5/exfoliated graphene were examined both in glass (Figure 7b) and PET substrate (Figure 7c), which showed transparent micro-supercapacitor device. Bending capabilities (Figure 7d) were also demonstrated with V_2O_5/exfoliated graphene composite at a bending angle of 0°, 30°, 60°, and 90°, where it was able to bend well under various bending angles. Furthermore, overall capacitance was maintained at different bending angles (0°, 30°, 60°, and 90°), which proved the sufficient flexibility and bendability of V_2O_5/exfoliated graphene composite-based micro-supercapacitor.

4.3. Integration of electrochromic supercapacitor with other devices

In addition to the structural advances in the flexible electrochromic supercapacitor, combination of flexible electrochromic supercapacitor with other energy harvesting devices was also devised. Qin et al. reported on the self-charging, flexible electrochromic supercapacitor that is combined with hybrid piezo/triboelectric generator,[82] which garnered significant

attention among the researchers. The hybrid nanogenerators composed of piezo/triboelectric components can generate a high output voltage of 150 V, which satisfies the self-charging requirements. As illustrated here, it is possible to combine other energy conversion method together with electrochromic supercapacitor to charge the supercapacitor while allowing it to operate. In other works, Zhang et al. reported on the solar-driven flexible electrochromic supercapacitor,[83] which is composed of dye-sensitized TiO_2 film and electrochromic WO_3 film. Some significant research works have taken place in the direction of combining flexible electrochromic supercapacitor with energy harvesters, such as piezoelectric/electrochromic supercapacitor for self-powered system[84] and tandem self-powered flexible electrochromic supercapacitor containing photovoltaics and triboelectric nanogenerator.[85] The overall electrochemical performance of flexible and/or stretchable electrochromic supercapacitor is summarized in Table 2.

5. Future Perspectives and Conclusion

In this review paper, the current status of electrochromic supercapacitor technology that can control the optical transmittance of the system while storing energy electrochemically is introduced. Existing electrochromic technology was mainly used for limited technologies such as smart window and low emission mirror. However, the electrochromic supercapacitor was developed since cathodic/anodic electrochromic materials that change color by inserting/desorption of electrolyte ions into the crystal have the same principle as the electrochemical charge/discharge reaction. This technology successfully overcomes the limitations of the limited application of conventional electrochromic and supercapacitors. Particularly, since it can be implemented as a smart-discoloration function that stores external power and visualizes an electrochemical reaction at the same time, it is mainly used in the development of next-generation energy storage systems that require various functions in addition to the energy storage function.

In the early stage of development, WO_3 and V_2O_5 transition metal oxides, which cause color change through bandgap change by electrochemical oxidation/reduction reaction, were mainly used. These materials successfully increased coloration contrast (coloration efficiency) and energy density but exhibited a slow coloration response time and low power density due to the low electrical conductivity of the material itself. To overcome such disadvantage, conductive polymers that have various oxidation/reduction sites and can control optical transmittance even if the narrow bandgap were utilized. Representatively, PEDOT:PSS, which has excellent electrical conductivity and is capable of cathodic coloration, was mainly used as an active material of high electrical conductivity-type. Recently, electrochromic-electrochemical performances have been optimized using hybrid-type composite active materials in which transition metal oxide and conductive polymer are combined.

The electrochromic supercapacitor is presented as an alternative to the next-generation energy storage system, but the scope of its use should be further expanded. First, it is necessary to combine with flexible-wearable electronics through the development of a wearable platform, but it still does not reach the performance of a glass-based electrochromic supercapacitor. Therefore, the development of transparent, flexible-stretchable substrates and electrolytes is necessary. Second, it should be expanded to a form of self-chargeable electrochromic supercapacitor that can store electric power produced from renewable energy, away from the form of storing external electric power. Supercapacitor has high power density, so it can quickly store/deliver electric energy produced from renewable energy. As the optical transmittance of the system can be freely adjusted, it is easy to converge with new and renewable energy technology using light. Through the extension of this electrochromic supercapacitor technology, it is expected that it will become a powerful alternative to the next-generation energy storage system.

Acknowledgements

This work was supported by funding from Bavarian Center for Battery Technology (Baybatt) and Bayerisch-Tschechische Hochschulagentur (BTHA) (BTHA-AP-2022-45). Open Access funding enabled and organized by Projekt DEAL.

Table 2. Summary of electrochemical performance on various types of flexible and/or stretchable electrochromic supercapacitor.

Active materials	Electrolyte	Capacitance	Coloration contrast	Cycling stability	Ref.
Cellulose/Ag/rGO/WO_3	1 M $LiClO_4$ in propylene carbonate	406.2 F g^{-1} at 0.5 A g^{-1}	41% at 600 nm	87.4% after 20000 cycles	[70]
Ag/PEDOT:PSS	PVA/LiCl in H_2O	443 F cm^{-3}	30% at 633 nm	Approximately 100% after 10000 cycles	[71]
CNTs/Au/PPy/PET	1 M $LiClO_4$ in H_2O	19.1 mF cm^{-2} at 10 mV s^{-1}	28.8% at 650 nm	79% after 1000 cycles	[75]
Polyaniline	0.5 M H_2SO_4 in ethanol	473.3F g^{-1} at 0.03Vs $^{-1}$	49% at 630 nm	77% after 1000 cycles	[76]
PI-IDT//$W_{0.71}Mo_{0.21}O_{3-x}$	0.5 M $LiClO_4$/PC	6.2 mF cm^{-2} at 0.05 mA cm^{-2}	21.84%	88% after 12500 cycles	[77]
PEDOT:PSS/WO_3	Polyacrylamid	471.0 F g^{-1}	37.7%	92.9% after 50000 cycles	[78]
PEDOT:PSS/AgNWs/WO_3	0.5 M H_2SO_4/10 wt% PVA	32.3 mAh g^{-1} at 2 A g^{-1}	40% at 633 nm	85% after 400 cycles	[80]
AgNWs/NiO	PVA/KOH	3.47 mF cm^{-2} at 2.0 μA cm^{-2}	≈15%	85.4% after 10000 cycles	[82]

Conflict of Interest

The authors declare no conflict of interest.

Data Availability Statement

The data that support the findings of this study are available from the corresponding author upon reasonable request.

[1] T. M. Gür, *Energy Environ. Sci.* **2018**, *11*, 2696.
[2] N. V. Gnanapragasam, B. V. Reddy, M. A. Rosen, *Int. J. Hydrocarbon Eng.* **2010**, *35*, 4788.
[3] G. Zhu, Z.-H. Lin, Q. Jing, P. Bai, C. Pan, Y. Yang, Y. Zhou, Z. L. Wang, *Nano Lett.* **2013**, *13*, 847.
[4] A. Khodabandehlo, A. Noori, M. S. Rahmanifar, M. F. El-Kady, R. B. Kaner, *Adv. Funct. Mater.* **2022**, *32*, 2204555. DOI: 10.1002/adfm.20220455.
[5] G. Shi, S. E. Lowe, A. J. T. Teo, T. K. Dinh, S. H. Tan, J. Qin, Y. Zhang, Y. L. Zhong, H. Zhao, *Appl. Mater. Today* **2019**, *16*, 482.
[6] Y. Pang, Z. Yang, Y. Yang, T.-L. Ren, *Small* **2019**, *16*, 1901124.
[7] H.-R. Lim, H. S. Kim, R. Qazi, Y.-T. Kwon, J.-W. Jeong, W.-H. Yeo, *Adv. Mater.* **2020**, *32*, 1901924.
[8] Q. Lyu, S. Gong, J. Yin, J. M. Dyson, W. Cheng, *Adv. Healthcare Mater.* **2021**, *10*, 2100577.
[9] T. Dinh, H.-P. Phan, T.-K. Nguyen, A. Qamar, A. R. M. Foisal, T. N. Viet, C.-D. Tran, Y. Zhu, N.-T. Nguyen, D. V. Dao, *J. Mater. Chem. C* **2016**, *4*, 10061.
[10] J. O. G. Posada, A. J. R. Rennie, S. P. Villar, V. L. Martins, J. Marinaccio, A. Barnes, C. F. Glover, D. A. Worsley, P. J. Hall, *Renewable Sustainable Energy Rev.* **2017**, *68*, 1174.
[11] B. Hu, C. DeBruler, Z. Rhodes, T. L. Liu, *J. Am. Chem. Soc.* **2017**, *139*, 1207.
[12] F. Zhang, W. Zhang, D. Wexler, Z. Guo, *Adv. Mater.* **2022**, *34*, 2107965.
[13] B. Hwang, J. Y. Cheong, P. Matteini, T. G. Yun, *Mater. Lett.* **2022**, *306*, 130954.
[14] D. Chao, W. Zhou, F. Xie, C. Ye, H. Li, M. Jaroniec, S.-Z. Qiao, *Sci. Adv.* **2020**, *6*, eaba4098.
[15] A. Borenstein, O. Hanna, R. Attias, S. Luski, T. Brousse, D. Aurbach, *J. Mater. Chem. A* **2017**, *5*, 12653.
[16] S. Najib, E. Erdem, *Nanoscale Adv.* **2019**, *1*, 2817.
[17] F. Wang, J. Y. Cheong, Q. He, G. Duan, S. He, L. Zhang, Y. Zhao, I.-D. Kim, S. Jiang, *Chem. Eng. J.* **2021**, *414*, 128767.
[18] C. Zhao, W. Zheng, *Front. Energy Res.* **2015**, *3*, 23.
[19] Y. Liu, Q. Wu, L. Liu, P. Manasa, L. Kang, F. Ran, *J. Mater. Chem. A* **2020**, *8*, 8218.
[20] J. Wang, F. Li, F. Zhu, O. G. Schmidt, *Small Methods* **2019**, *3*, 1800367.
[21] K. Wang, W. Zou, B. Quan, A. Yu, H. Wu, P. Jiang, Z. Wei, *Adv. Energy Mater.* **2011**, *1*, 1068.
[22] J. Ren, L. Li, C. Chen, X. Chen, Z. Cai, L. Qiu, Y. Wang, X. Zhu, H. Peng, *Adv. Mater.* **2013**, *25*, 1155.
[23] Y. Wang, X. Wu, Y. Han, T. Li, *J. Energy Storage* **2021**, *42*, 103053.
[24] Y. Ko, M. Kwon, W. K. Bae, B. Lee, S. W. Lee, J. Cho, *Nat. Commun.* **2017**, *8*, 536.
[25] C. Choi, J. A. Lee, A. Y. Choi, Y. T. Kim, X. Lepró, M. D. Lima, R. H. Baughman, S. J. Kim, *Adv. Mater.* **2014**, *26*, 2059.
[26] D. P. Dubal, N. R. Chodanker, D.-H. Kim, P. Gomez-Romero, *Chem. Soc. Rev.* **2018**, *47*, 2065.
[27] K. Keum, J. W. Kim, S. Y. Hong, J. G. Son, S.-S. Lee, J. S. Ha, *Adv. Mater.* **2020**, *32*, 2002180.
[28] S. Wang, H. Xu, T. Hao, M. Xu, J. Xue, J. Zhao, Y. Li, *Appl. Surf. Sci.* **2022**, *577*, 151889.
[29] W. Xinming, W. Qiguan, Z. Wenzhi, W. Yan, C. Weixing, *J. Mater. Sci.* **2016**, *51*, 7731.
[30] W. Wei, X. Cui, W. Chen, D. G. Ivey, *Chem. Soc. Rev.* **2011**, *40*, 1697.
[31] Y.-H. Lee, J. S. Kang, J.-H. Park, J. Kang, I.-R. Jo, Y.-E. Sung, K.-S. Ahn, *Nano Energy* **2020**, *72*, 104720.
[32] G. Zhang, J. Hu, Y. Nie, Y. Zhao, L. Wang, Y. Li, H. Liu, L. Tang, X. Zhang, D. Li, L. Sun, H. Duan, *Adv. Funct. Mater.* **2021**, *31*, 2100290.
[33] S. Yoon, E. Kang, J. K. Kim, C. W. Lee, J. Lee, *Chem. Commun.* **2011**, *47*, 1021.
[34] Z. Fang, Y. Yin, X. Qiu, L. Zhu, X. Dong, Y. Wang, Y. Xia, *Adv. Energy & Sustainable Res.* **2021**, *2*, 2100105.
[35] V. Augustyn, P. Simon, B. Dunn, *Energy Environ. Sci.* **2014**, *7*, 1597.
[36] A. M. Bryan, L. M. Santino, Y. Lu, S. Acharya, J. M. D'Arcy, *Chem. Mater.* **2016**, *28*, 5989.
[37] R. Song, G. Li, Y. Zhang, B. Rao, S. Xiong, G. He, *Chem. Eng. J.* **2021**, *422*, 130057.
[38] H. Yue, X. Ju, Y. Du, Y. Zhang, H. Du, J. Zhao, J. Zhang, *Org. Electron.* **2021**, *95*, 106183.
[39] D. Ma, G. Shi, H. Wang, Q. Zhang, Y. Li, *J. Mater. Chem. A* **2013**, *1*, 684.
[40] D. Choi, M. Son, T. Im, S.-H. Ahn, C. S. Lee, *Mater. Chem. Phys.* **2020**, *249*, 123121.
[41] S. Fleischmann, J. B. Mitchell, R. Wang, C. Zhan, D.-e. Jiang, V. Presser, V. Augustyn, *Chem. Rev.* **2020**, *120*, 6738.
[42] D. Wei, M. R. J. Scherer, C. Bower, P. Andrew, T. Ryhänen, U. Steiner, *Nano Lett.* **2012**, *12*, 1857.
[43] M. M. J. Scherer, U. Steiner, *Nano Lett.* **2013**, *13*, 3005.
[44] G. Cai, X. Wang, M. Cui, P. Darmawan, J. Wang, A. L.-S. Eh, P. S. Lee, *Nano Energy* **2015**, *12*, 258.
[45] T. Y. Yun, X. Li, S. H. Kim, H. C. Moon, *ACS Appl. Mater. Interfaces* **2018**, *10*, 43993.
[46] M. Kandasamy, S. Sahoo, S. K. Nayak, B. Chakraborty, C. S. Rout, *J. Mater. Chem. A* **2021**, *9*, 17643.
[47] G. Santhosh, G. P. Nayaka, A. S. Bhatt, *J. Alloys Compd.* **2022**, *899*, 163312.
[48] S. Zhou, S. Wang, S. Zhou, H. Xu, J. Zhao, J. Wang, Y. Li, *Nanoscale* **2020**, *12*, 8934.
[49] A. K. Prasad, J.-Y. Park, S.-H. Kang, K.-S. Ahn, *Electrochim. Acta* **2022**, *422*, 140340.
[50] H. S. Chavan, B. Hou, Y. Jo, A. I. Inamdar, H. Im, H. Kim, *ACS Appl. Mater. Interfaces* **2021**, *13*, 57403.
[51] J. Li, A. Levitt, N. Kurra, K. Juan, N. Noriega, X. Xiao, X. Wang, H. Wang, H. N. Alshareef, Y. Gogotsi, *Energy Storage Mater.* **2019**, *20*, 455.
[52] J. Cho, T. Y. Yun, H. Y. Noh, S. H. Baek, M. Nam, B. Kim, H. C. Moon, D.-H. Ko, *Adv. Funct. Mater.* **2020**, *30*, 1909601.
[53] B. Ezhilmaran, S. V. Bhat, *Chem. Eng. J.* **2022**, *446*, 136924.
[54] X.-A. Liu, J. Wang, D. Tang, Z. Tong, H. Ji, H.-Y. Qu, *J. Mater. Chem. A* **2022**, *10*, 12643.
[55] D. Mohanadas, N. H. N. Azman, Y. Sulaiman, *J. Energy Storage* **2022**, *48*, 103954.
[56] M. Hassan, G. Abbas, Y. Lu, Z. Wang, Z. Peng, *J. Mater. Chem. A* **2022**, *10*, 4870.
[57] W. Li, J. Zhang, Y. Zheng, Y. Cui, *Sol. Energy Mater. Sol. Cells* **2022**, *235*, 111488.
[58] B. Safdar, A. K. Prasad, K.-S. Ahn, *Chem. Phys. Lett.* **2021**, *783*, 139024.
[59] B. Wang, Q. Li, H. Zou, Q. Guo, G. Nie, *J. Polym. Sci.* **2021**, *59*, 3100.
[60] S. Deshagani, D. Maity, A. Das, M. Deepa, *ACS Appl. Mater. Interfaces* **2021**, *13*, 34518.
[61] J. Xue, H. Xu, S. Wang, T. Hao, Y. Yang, X. Zhang, Y. Song, Y. Li, J. Zhao, *Appl. Surf. Sci.* **2021**, *565*, 150512.
[62] Z. Li, B. Wang, X. Zhao, Q. Guo, G. Nie, *New J. Chem.* **2020**, *44*, 20584.
[63] Y. Wang, X. Jia, M. Zhu, X. Liu, D. Chao, *New J. Chem.* **2020**, *44*, 8138.
[64] Q. Guo, J. Li, B. Zhang, G. Nie, D. Wang, *ACS Appl. Mater. Interfaces* **2019**, *11*, 6491.
[65] Z. Xie, X. Jin, G. Chen, J. Xu, D. Chen, G. Shen, *Chem. Commun.* **2014**, *50*, 608.
[66] K. Wang, H. Wu, Y. Meng, Y. Zhang, Z. Wei, *Energy Environ. Sci.* **2012**, *5*, 8384.
[67] M. Zhu, Y. Huang, Y. Huang, W. Meng, Q. Gong, G. Li, C. Zhi, *J. Mater. Chem. A* **2015**, *3*, 21321.
[68] X. Chen, H. Lin, J. Deng, Y. Zhang, X. Sun, P. Chen, X. Fang, Z. Zhang, G. Guan, H. Peng, *Adv. Mater.* **2014**, *26*, 8126.
[69] G. Cai, P. Darmawan, M. Cui, J. Wang, J. Chen, S. Magdassi, P. S. Lee, *Adv. Energy Mater.* **2016**, *6*, 1501882.
[70] T. G. Yun, D. Kim, Y. H. Kim, M. Park, S. Hyun, S. M. Han, *Adv. Mater.* **2017**, *29*, 1606728.
[71] R. T. Ginting, M. M. Ovhal, J.-W. Kang, *Nano Energy* **2018**, *53*, 650.
[72] Y. Guo, W. Li, H. Yu, D. F. Perepichka, H. Meng, *Adv. Energy Mater.* **2017**, *7*, 1601623.
[73] L. Shen, L. Du, S. Tan, Z. Zang, C. Zhao, W. Mai, *Chem. Commun.* **2016**, *52*, 6296.
[74] F. Grote, Z.-Y. Yu, J.-L. Wang, S.-H. Yu, Y. Lei, *Small* **2016**, *36*, 4666.
[75] X. Jiao, G. Li, Z. Yuan, C. Zhang, *ACS Appl. Energ. Mater.* **2021**, *4*, 14155.
[76] K. Zhou, H. Wang, J. T. Liu, J. Liu, H. Yan, K. Suganuma, *Chem. Eng. J.* **2018**, *345*, 290.

[77] Y. Sun, Y. Zhao, G. Zhu, M. Li, X. Zhang, H. Yang, B. Lin, *Electrochim. Acta* **2020**, *333*, 135495.
[78] T. G. Yun, M. Park, D.-H. Kim, D. Kim, J. Y. Cheong, J. G. Bae, S. M. Han, I.-D. Kim, *ACS Nano* **2019**, *13*, 3141.
[79] T. An, Y. Ling, S. Gong, B. Wen, Y. Zhao, D. Dong, L. W. Yap, Y. Wang, W. Cheng, *Adv. Mater. Technol.* **2019**, *4*, 1800473.
[80] G. Cai, S. Park, X. Cheng, A. L.-S. Eh, P. S. Lee, *Sci. Technol. Adv. Mater.* **2018**, *19*, 759.
[81] P. Zhang, F. Zhu, F. Wang, J. Wang, R. Dong, X. Zhuang, O. G. Schmidt, X. Feng, *Adv. Mater.* **2017**, *29*, 1604491.
[82] S. Qin, Q. Zhang, X. Yang, M. Liu, Q. Sun, Z. L. Wang, *Adv. Energy Mater.* **2018**, *8*, 1800069.
[83] D. Zhang, B. Sun, H. Huang, Y. Gan, Y. Xia, C. Liang, W. Zhang, J. Zhang, *Materials* **2020**, *13*, 1206.
[84] Z. He, B. Gao, T. Li, J. Liao, B. Liu, X. Liu, C. Wang, Z. Feng, Z. Gu, *ACS Sustainable Chem. Eng.* **2019**, *7*, 1745.
[85] J. Huang, Z. Ren, Y. Zhang, P. W.-K. Fong, H. T. Chandran, Q. Liang, K. Yao, H. Tang, H. Xia, H. Zhang, X. Yu, Z. Zheng, G. Li, *Adv. Energy Mater.* **2022**, *12*, 2201042.

Manuscript received: October 17, 2022
Revised manuscript received: December 14, 2022
Accepted manuscript online: December 15, 2022
Version of record online: January 9, 2023